AIAA JOURNAL
Vol. 52, No. 5, May 2014

Technical Notes

Analytical Solutions of Shock Structure Thickness and Asymmetry in Navier–Stokes/Fourier Framework

R. S. Myong*
Gyeongsang National University, Gyeongnam 660-701, Republic of Korea

DOI: 10.2514/1.J052583

Nomenclature

C	=	integration constant
C_v	=	specific heat at constant volume
E	=	internal energy
l	=	mean free path based on mass flux
M	=	Mach number
O	=	mass flux
P	=	total momentum flux
p	=	thermodynamic pressure
Q	=	total energy flux
Q_s	=	shock asymmetry
Q_x	=	x component of heat flux vector
R	=	gas constant
r	=	dimensionless density
s	=	exponent of the inverse power laws
T	=	temperature
u	=	x component of velocity vector
v	=	dimensionless velocity
x	=	coordinate normal to the shock front
$\bar{x}$	=	dimensionless coordinate normal to the shock front
α	=	parameter of upstream Mach number
γ	=	specific heat ratio
Δ	=	temperature–density separation distance
δ	=	shock thickness
η	=	viscosity
θ	=	dimensionless temperature
κ	=	thermal conductivity
λ	=	mean free path
μ	=	parameter of upstream Mach number
ξ	=	dimensionless coordinate
Π_{xx}	=	xx component of stress tensor
ρ	=	density
σ	=	dimensionless stress
ϕ	=	dimensionless pressure
φ	=	dimensionless heat flux
Ψ	=	dimensionless nonequilibrium entropy

Received 6 February 2013; revision received 18 April 2013; accepted for publication 4 October 2013; published online 20 February 2014.

*Professor, Department of Aerospace and System Engineering and Research Center for Aircraft Parts Technology, Jinju; myong@gnu.ac.kr. Associate Fellow AIAA.

I. Introduction

THE problem of shock wave structures of gases is not only important from the technological viewpoint, but it has also been a major stumbling block for theoreticians for a long time [1–7]. For example, the shock wave structures have a big impact on the overall flow patterns around hypersonic aerospace vehicles flying at high altitude [8]. The stationary shock wave structure is defined as a very thin (order of mean free path) stationary gas flow region between the supersonic upstream and subsonic downstream [9–11].

There are at present two theoretical issues regarding this rather simple physical problem. The first issue concerns the physics of shock wave structures for varying Mach numbers, such as shock thickness and asymmetry [1–3,6,7,12–17]. In addition, the derivation of proper hydrodynamic equations valid in very high Mach numbers is a hot research topic in nonequilibrium gas dynamics [4–7]. The second issue is the numerical difficulty associated with the stiffness of the shock structure arising from the rapid change of physical properties in the extremely thin region. It is well known that the stiff shock structure is one of the toughest problems to solve numerically, either in the system of ordinary differential equations [6,18] or in the form of partial differential equations [18–22]. It was further noted that numerical results of the shock structure are found to be very sensitive to the extent of the computational domain, the imposed downstream boundary conditions, the level of intrinsic viscosity and thermal conductivity, physical and artificial, and the employed time integration schemes and so on [22], making the verification and validation study very challenging [23].

This Note presents analytical solutions, in particular, the asymmetry and temperature–density separation, to the shock structure problem in elementary function form within the Navier–Stokes/Fourier framework. These results, which do not seem to have been derived in the past, are not only useful in the study of the physics of the shock inner structure but also in the verification of the computational fluid dynamics scheme.

II. Analytical Solutions in Closed Form

The conservation laws for the one-dimensional shock wave structure and the equation of state can be written as

$$\begin{aligned} &\rho u = O, \\ &\rho u^2 + p + \Pi_{xx} = P, \\ &\rho u\left(E + \frac{1}{2}u^2\right) + u(p + \Pi_{xx}) + Q_x = Q, \\ &p = \rho RT \end{aligned} \tag{1}$$

where O, P, and Q are integration constants for mass, momentum, and total energy, respectively. It should be mentioned that the conservation laws are the direct consequence of the kinetic Boltzmann equation and are valid for all the flow regimes. When the following Navier–Stokes/Fourier constitutive relations are inserted into the conservation laws,

$$\Pi_{xx} = -\frac{4}{3}\eta\frac{\mathrm{d}u}{\mathrm{d}x}, \qquad Q_x = -\kappa\frac{\mathrm{d}T}{\mathrm{d}x} \tag{2}$$

and, after introducing the following dimensionless parameters based on the conserved properties O, P, and Q, which turned out to be crucial in deriving analytical solutions in closed form in a more efficient way,

$$r = \rho O^{-2} P, \quad v = uOP^{-1}, \quad \phi = pP^{-1}, \quad \theta = RTO^2 P^{-2},$$
$$\sigma = \Pi_{xx} P^{-1}, \quad \varphi = Q_x Q^{-1}, \quad \xi = xl^{-1}, \quad \alpha = OP^{-2} Q \quad (3)$$

the equations are reduced to ($E = 3RT/2$)

$$\begin{aligned} &rv = 1, \\ &rv^2 + \phi + \sigma = 1, \\ &v^2 + 5\theta + 2\sigma v + 2\alpha\varphi = 2\alpha, \\ &\phi = r\theta \end{aligned} \quad (4)$$

and

$$\sigma = -\frac{4}{3}\eta^* \frac{\mathrm{d}v}{\mathrm{d}\xi}, \qquad \varphi = -\frac{5}{2}\kappa^* \frac{\theta_1}{\alpha Pr} \frac{\mathrm{d}\theta}{\mathrm{d}\xi} \quad (5)$$

where ξ represents a dimensionless length scale based on the upstream (subscript 1) mean free path l

$$\xi = \frac{x}{l}, \qquad l = \frac{\eta_1}{\rho_1 u_1}$$

Here the reduced viscosity η^* and thermal conductivity κ^* can be expressed in terms of θ and s, which are related to the exponent of the inverse power laws of gas molecules,

$$\eta^* = \left(\frac{\theta}{\theta_1}\right)^s, \qquad \kappa^* = \left(\frac{\theta}{\theta_1}\right)^s$$

The spatial coordinate ξ is also related to $\bar{x}$ the length scale based on an effective mean free path λ:

$$\xi = \bar{x}\left(\sqrt{\frac{\gamma\pi}{2}} M\right), \qquad \bar{x} = \frac{x}{\lambda} = \frac{x}{\sqrt{\pi/2}\eta_1/(\rho_1\sqrt{RT_1})}$$

Here M and γ are the upstream Mach number and the specific heat ratio, respectively. It can be further noted that the parameter α introduced in Eq. (3) is basically a function of the upstream Mach number

$$\alpha = \frac{\gamma^2 M^2[2 + (\gamma - 1)M^2]}{2(\gamma - 1)(1 + \gamma M^2)^2}$$

In addition, the following boundary conditions, which are nothing but the Rankine–Hugoniot relations, can be derived by applying σ, $\varphi(\xi = \pm\infty) = 0$ to Eq. (4):

$$r_{1,2} = \frac{1}{v_{1,2}} = \frac{8}{5 \pm \mu}, \qquad \phi_{1,2} = \frac{3 \mp \mu}{8}, \qquad \theta_{1,2} = \frac{15 \mp 2\mu - \mu^2}{64} \quad (6)$$

where

$$\mu = \sqrt{25 - 32\alpha}$$

Here the upper sign is for the upstream 1 and the lower sign is for the downstream 2. Equations (4) and (5) can be simplified into the following differential equation:

$$v^2 + 5\theta - 2\alpha - \frac{4}{3}\eta^* \frac{\mathrm{d}}{\mathrm{d}\xi}\left[v^2 + \frac{3/4}{Pr}(5\theta)\right] = 0 \quad (7)$$

There is no known general analytic solution to this nonlinear differential equation, but they can be integrated in the case of $Pr = 3/4$, which is a good approximation for the actual value of many gases including air ($Pr = 0.72$). It then reduces to an integrable form

$$v^2 + 5\theta - 2\alpha - \frac{4}{3}\eta^* \frac{\mathrm{d}}{\mathrm{d}\xi}(v^2 + 5\theta - 2\alpha) = 0 \quad (8)$$

Note that a term $\mathrm{d}(2\alpha)/\mathrm{d}\xi = 0$ is added in the process. The solution is

$$v^2 + 5\theta - 2\alpha = C \exp\left(\frac{3}{4}\int_{-\infty}^{\xi} \frac{1}{\eta^*}\,\mathrm{d}\xi\right)$$

where C is an integration constant. It turns out that the constant must be zero to have a physically allowable solution; otherwise, the total energy density of the gas would vary exponentially with spatial coordinate. Thus, we can derive a simple form of the energy conservation law

$$v^2 + 5\theta - 2\alpha = 0 \quad (9)$$

By combining the momentum conservation law in Eq. (4) and the Navier constitutive relation in Eq. (5) with the new form of energy conservation Eq. (9), we can derive a differential equation for the shock wave inner structure:

$$\frac{5}{3}\eta^* v \frac{\mathrm{d}v}{\mathrm{d}\xi} = v^2 - \frac{5}{4}v + \frac{\alpha}{2} \quad (10)$$

By noting $\eta^* = (2\alpha - v^2)^s/(5\theta_1)^s$ and recalling the fact that the right-hand term can be factored into $(v - v_1)(v - v_2)$, the equation reduces to a nonlinear differential equation of the velocity $v(\xi)$ only

$$\frac{\mathrm{d}v}{\mathrm{d}\xi} = \frac{3}{5}(5\theta_1)^s \frac{(v - v_1)(v - v_2)}{v(2\alpha - v^2)^s} \quad (11)$$

A. Inverse Shock Density Thickness

Equation (11) can provide the shock thickness based on the maximum slope of the velocity in the shock profile. However, the density, not the velocity, is measured in the experimental investigation of the shock structure [13,14]. Therefore, Eq. (11) needs to be transformed into the following differential equation of the density $r(\xi)$

$$\frac{\mathrm{d}r}{\mathrm{d}\xi} = \frac{3}{5}(5\theta_1)^s \frac{r(r - r_1)(r_2 - r)}{r_1 r_2 (2\alpha - r^{-2})^s} \quad (12)$$

By noting that $\mathrm{d}r/\mathrm{d}\xi$ becomes maximum at the location ξ satisfying

$$6\alpha^2 r^4 - 10\alpha r^3 + \alpha(1 - 2s)r^2 + 5(s + 1)r - 2(2s + 1) = 0 \quad (13)$$

the maximum slope can be determined without actually solving the differential Eq. (12). A unique real root of the quartic equation of r ($r_1 < r < r_2$) can always be obtained by Ferrari's method [24]. The inverse shock density thickness δ is then calculated by

$$\delta^{-1} = \sqrt{\frac{\gamma\pi}{2}} \frac{M}{r_2 - r_1} \left(\frac{\mathrm{d}r}{\mathrm{d}\xi}\right)_{\max} \quad (14)$$

B. Shock Structure Asymmetry

In contrast to the case of the thickness, the exact profile within the shock structure is necessary to determine other shock wave properties such as the asymmetry. The simplest case $s = 0$ in the nonlinear differential equation of the velocity $v(\xi)$ [Eq. (11)], constant coefficients of viscosity and conductivity, was already solved analytically in the previous study [3]. The possibility of deriving the analytical solutions in closed form in the case of the Maxwellian molecule ($s = 1$) and the hard sphere ($s = 1/2$) has been, however, overlooked in the past, probably due to the rather complicated form of the nonlinear differential Eq. (11). Here the analytic solution to the Maxwellian molecule is first presented in closed form, because it is simpler in the mathematical sense and, at the same time, it preserves

the essence of behaviors inherent in general molecules. By recognizing the following integral formula,

$$\int \frac{v(2\alpha - v^2)}{(v - v_1)(v - v_2)}\,\mathrm{d}v = -(v_1 + v_2)v - \frac{1}{2}v^2 + \frac{1}{v_1 - v_2}\ln\frac{(v_1 - v)^{v_1(2\alpha - v_1^2)}}{(v - v_2)^{v_2(2\alpha - v_2^2)}}$$

the following differential equation can be integrated analytically:

$$\frac{3}{5}(5\theta_1)\mathrm{d}\xi = \frac{v(2\alpha - v^2)}{(v - v_1)(v - v_2)}\mathrm{d}v$$

That is, by choosing the proper integration constant related to the physical location of the shock wave and also by noting $r(x) = 1/v(x)$, the *implicit* density solution $r(x)$ in the range of $r_1 < r < r_2$ can be derived in a compact functional form:

$$3\theta_1 M\sqrt{\frac{\gamma\pi}{2}}\bar{x} = \frac{1}{r_a}\left(\frac{5}{4} + \frac{1}{2r_a}\right) - \frac{1}{r}\left(\frac{5}{4} + \frac{1}{2r}\right) + \frac{4}{\mu}\ln\frac{[(r_1^{-1} - r^{-1})/(r_1^{-1} - r_a^{-1})]^{(2\alpha - r_1^{-2})/r_1}}{[(r^{-1} - r_2^{-1})/(r_a^{-1} - r_2^{-1})]^{(2\alpha - r_2^{-2})/r_2}} \tag{15}$$

Here the integration constant is determined by the arithmetic mean of the upstream and downstream density

$$r_a = \frac{1}{2}(r_1 + r_2) = \frac{5}{4\alpha}$$

which is equivalent to the harmonic mean of the upstream and downstream velocity. Note that the choice of the integration constant is not unique; for example, in the previous study [3], the constant was chosen such that the inflection point, that is, the point with maximum velocity slope, may coincide with the origin of the coordinate $x = 0$. For the known density profile (15), the shock asymmetry introduced by Schmidt [13] can be expressed as follows:

$$Q_s = \frac{\int_{-\infty}^{0}(r(x) - r_1)\,\mathrm{d}x}{\int_{0}^{\infty}(r_2 - r(x))\,\mathrm{d}x} = \frac{\int_{r_a}^{r_1} x(r)\,\mathrm{d}r}{\int_{r_a}^{r_2} x(r)\,\mathrm{d}r} = \frac{-(\mu/4)[(5/4)\ln(r_1/r_a) - (1/2)((1/r_1) - (1/r_a)) - (1/r_a)((5/4) + (1/2r_a))(r_1 - r_a)] - (5/4)((1/r_2) - (1/r_1))\ln(r_1/r_a) - (2\alpha - (1/r_2^2))(1 - (r_1/r_2))\ln((r_a^{-1} - r_2^{-1})/(r_1^{-1} - r_2^{-1}))}{-(\mu/4)[(5/4)\ln(r_2/r_a) - (1/2)((1/r_2) - (1/r_a)) - (1/r_a)((5/4) + (1/2r_a))(r_2 - r_a)] - (5/4)((1/r_2) - (1/r_1))\ln(r_2/r_a) - (2\alpha - (1/r_1^2))((r_2/r_1) - 1)\ln((r_1^{-1} - r_a^{-1})/(r_1^{-1} - r_2^{-1}))} \tag{16}$$

Note that a new technique, the exchange of variables $r(x)$, $x(r)$ in integrand, is needed to derive the asymmetry in closed form. That is, for the implicit density solution (15) in the form of $x = F(1/r)$ or $1/r = F^{-1}(x)$, the integral $\int r(x)\,\mathrm{d}x = \int 1/F^{-1}(x)\,\mathrm{d}x$ in the asymmetry can be reduced into an analytically solvable form $\int F(1/r)\,\mathrm{d}r$ because the area defined by an integration

$$\int_0^{\infty}(r_2 - r(x))\,\mathrm{d}x$$

is equal to the area defined by an integration

$$\int_{r_a}^{r_2} x(r)\,\mathrm{d}r$$

in the present *monotonic* shock profile bounded by r_1 and r_2. In this process, the following integral formula has been used:

$$\int\left(\int \frac{v(2\alpha - v^2)}{(v - v_1)(v - v_2)}\,\mathrm{d}v\right)\mathrm{d}r = \frac{1}{2r} - (r_1^{-1} + r_2^{-1})\ln r + \frac{2\alpha - r_1^{-2}}{r_1^{-1} - r_2^{-1}}(r_1^{-1}r - 1)\ln(r_1^{-1} - r^{-1}) - \frac{2\alpha - r_2^{-2}}{r_1^{-1} - r_2^{-1}}(r_2^{-1}r - 1)\ln(r_2^{-1} - r^{-1})$$

In addition, the shock asymmetry has the following asymptotics for upstream Mach number M:

$$Q_{s_{M\to 1}} = 1, \qquad Q_{s_{M\to\infty}} = \frac{125}{106}\ln 5 - \frac{38}{53} \doteq 1.181$$

C. Shock Temperature–Density Separation

Until now, no investigations of temperature (or pressure) profiles in the shock inner structure have been conducted. Another parameter, the so-called the shock temperature–density separation, can be considered. It measures the separation distance between density and temperature profiles and can be easily calculated as follows: In conjunction with Eqs. (9) and (15),

$$\Delta = \bar{x}(r_a) - \bar{x}(r(\theta_a)) = -\bar{x}(r(\theta_a)) \quad \text{where } r(\theta_a) = \left(\frac{32}{25 - 16\alpha}\right)^{1/2} \text{ and } \theta_a = \frac{\theta_1 + \theta_2}{2} \tag{17}$$

The shock separation distance has the following asymptotics:

$$\Delta_{M\to 1} = \frac{1}{2}\sqrt{\frac{30}{\pi}} \doteq 1.545, \qquad \Delta_{M\to\infty} \to \infty$$

D. Other Profiles

Once the density and velocity profiles are known, all other solutions, including nonconserved variables, the stress, the heat flux, and the nonequilibrium entropy distribution $\hat{\Psi}$ [6], can be derived using the following relations:

$$\theta = \frac{2\alpha - v^2}{5}, \quad \phi = \frac{2\alpha - v^2}{5v}, \quad \sigma = -\frac{4v^2 - 5v + 2\alpha}{5v}, \quad \varphi = \frac{4v^2 - 5v + 2\alpha}{5\alpha},$$
$$\frac{\hat{\Psi} - \hat{\Psi}_1}{C_v} = \ln\frac{\theta}{\theta_1} + (\gamma - 1)\ln\frac{r_1}{r} - \frac{\gamma - 1}{4}\left(\bar{\sigma}^2 + \frac{2\gamma}{\gamma - 1}\bar{\varphi}^2\right) \tag{18}$$

where two additional parameters of the normal stress and the heat flux are introduced:

$$\bar{\sigma} = \frac{\sigma}{\phi}, \qquad \bar{\varphi} = \frac{\gamma - 1}{\gamma}\frac{\alpha\varphi}{\phi\sqrt{\theta}} \tag{19}$$

III. Results

The analytical solutions expressed in terms of r, v, and θ can be transformed in terms of ρ, u, and T properties

$$r = \rho O^{-2} P = \frac{\rho}{\rho_1}\left(1+\frac{1}{M^2}\right), \qquad v = uOP^{-1} = \frac{u}{u_1}\left(1+\frac{1}{M^2}\right)^{-1},$$
$$\theta = RTO^2P^{-2} = \frac{T}{T_1}\frac{1}{\gamma M^2}\left(1+\frac{1}{M^2}\right)^{-2}$$

When the normalized variables [e.g., $\bar{r} \equiv (r-r_1)/(r_2-r_1)$] are introduced, then it can be shown that

$$\bar{r} = \bar{\rho}, \qquad \bar{v} = \bar{u}, \qquad \bar{\theta} = \bar{T}$$

In Figs. 1 and 2, the shock structure profiles of conserved and nonconserved variables in the case of a high Mach number 15 are illustrated for different molecules. A noticeable feature is that the shock transition regime extends further to upstream as the molecule deviates from the Maxwellian type. In the case of a Maxwellian molecule, there exists a rapid transition at the upstream front starting near the location $x/\lambda = -10$. Another feature can be found in Fig. 3 of the stress and heat flux in the phase plane (σ, φ): The phase portraits remain essentially the same for a given Mach number regardless of the molecule type. In Figs. 4–6, the main profile characteristics of the shock inner structure are illustrated for varying

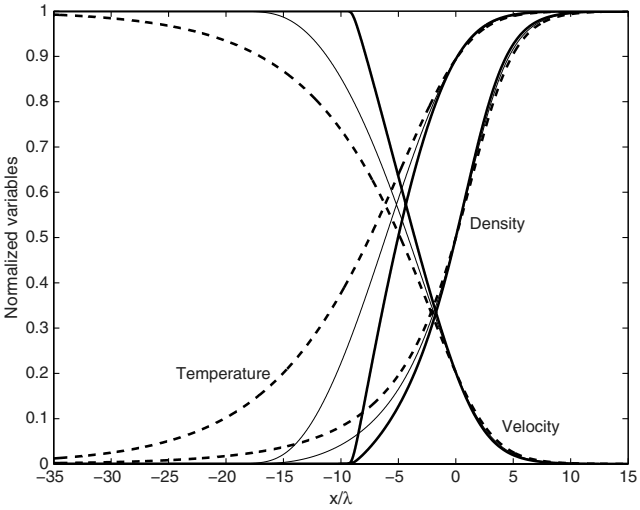

Fig. 1 Shock structure profiles ($M = 15$). Maxwellian molecule ($s = 1$) for the thick solid curve; hard sphere ($s = 1/2$) for the thin solid curve; constant case ($s = 0$) for the broken curve.

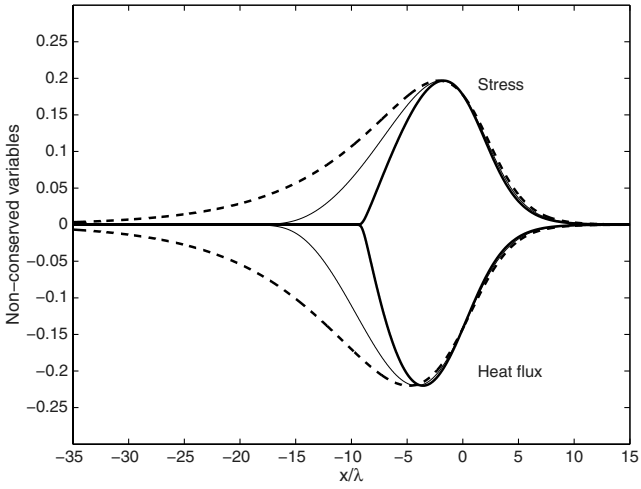

Fig. 2 Stress σ vs heat flux φ ($M = 15$). Maxwellian molecule ($s = 1$) for the thick solid curve; hard sphere ($s = 1/2$) for the thin solid curve; constant case ($s = 0$) for the broken curve.

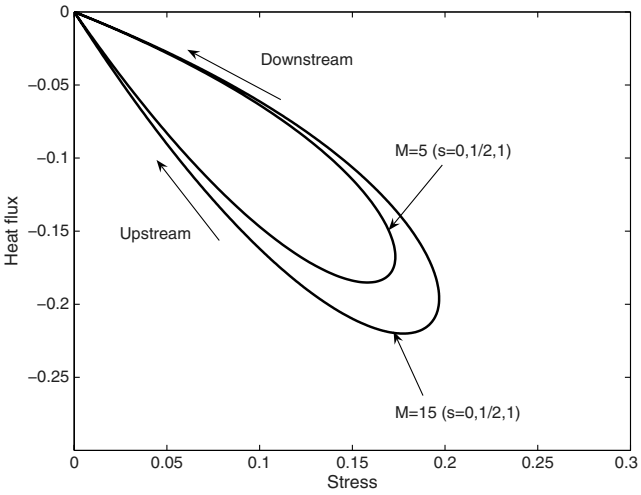

Fig. 3 Stress σ and heat flux φ in the phase plane.

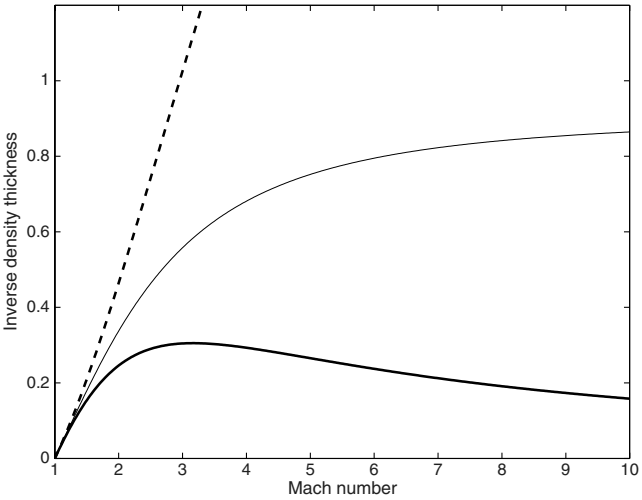

Fig. 4 Inverse shock density thickness. Maxwellian molecule ($s = 1$) for the thick solid curve; hard sphere ($s = 1/2$) for the thin solid curve; constant case ($s = 0$) for the broken curve.

Mach numbers. It can be observed that molecules close to the Maxwellian type show nonmonotonic behavior in the thickness, whereas molecules with small value of s do not show any finite asymptotic behavior for increasing Mach numbers. It is also shown

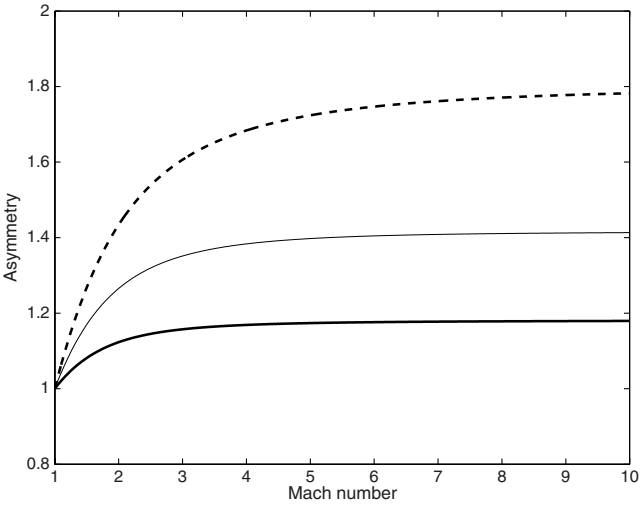

Fig. 5 Shock asymmetry. Maxwellian molecule ($s = 1$) for the thick solid curve; hard sphere ($s = 1/2$) for the thin solid curve; constant case ($s = 0$) for the broken curve.

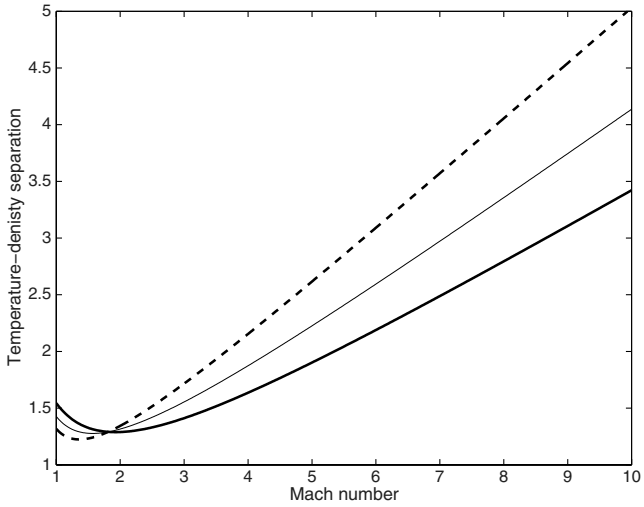

Fig. 6 Shock temperature–density separation. Maxwellian molecule ($s = 1$) for the thick solid curve; hard sphere ($s = 1/2$) for the thin solid curve; constant case ($s = 0$) for the broken curve.

that the asymptotic values of the Maxwellian molecule and hard sphere are 0.0 and 0.9076, respectively. On the other hand, the shock asymmetry is qualitatively similar for all molecules as shown in Fig. 5. All molecules have $Q_s = 1$ in $M = 1$ limit, but have different asymptotic values in infinite Mach number limit, with the Maxwellian molecule showing the smallest asymmetry. Finally, the shock temperature–density separation distance is shown in Fig. 6. The shock separation is not monotonic for all molecules and it continuously increases for increasing Mach numbers after a critical Mach number. Interestingly, the shock distances coincide at a particular Mach number $M = 1.811$ ($\Delta = 1.29$) for $s = 0, 1/2, 1$, which does not seem to have been identified previously.

IV. Conclusions

Closed-form analytical formulas (12–19) and (A1–A4) for the shock wave structure in monatomic gases are derived within the Navier–Stokes/Fourier framework. In particular, the shock thickness and asymmetry requiring the spatial differentiation and integral of density profile, respectively, are presented in elementary function form. In the derivation, the only major assumption introduced is a special value of a Prandtl number of three-fourths. These fully analytical results are expected to benefit the better understanding of the shock inner structure physics for all Mach numbers and the verification of the numerical scheme.

Appendix A: Other Molecular Cases

A1 Hard Sphere Case

The analytic solution to the hard sphere ($s = 1/2$) can also be derived in closed form. By recognizing the following integral formula,

$$\int \frac{v(2\alpha - v^2)^{1/2}}{(v - v_1)(v - v_2)}\,\mathrm{d}v = (2\alpha - v^2)^{1/2} - (v_1 + v_2)\tan^{-1}\frac{v}{(2\alpha - v^2)^{1/2}} - \frac{v_1(2\alpha - v_1^2)^{1/2}}{v_1 - v_2}\tanh^{-1}\frac{(2\alpha - v_1^2)^{1/2}(2\alpha - v^2)^{1/2}}{2\alpha - v_1 v} + \frac{v_2(2\alpha - v_2^2)^{1/2}}{v_1 - v_2}\tanh^{-1}\frac{(2\alpha - v_2^2)^{1/2}(2\alpha - v^2)^{1/2}}{2\alpha - v_2 v}$$

the implicit density solution can be derived in a compact functional form:

$$3\theta_1 M\sqrt{\frac{\gamma\pi}{2}}(2\alpha - r^{-2})^{1/2} - (2\alpha - r_a^{-2})^{1/2} + \frac{5}{4}(\tan^{-1}(2\alpha r_a^2 - 1)^{-1/2} - \tan^{-1}(2\alpha r^2 - 1)^{-1/2}) + \frac{4}{\mu}r_1^{-1}(2\alpha - r_1^{-2})^{1/2}\left(\tanh^{-1}\frac{(2\alpha - r_1^{-2})^{1/2}(2\alpha - r_a^{-2})^{1/2}}{2\alpha - r_1^{-1}r_a^{-1}} - \tanh^{-1}\frac{(2\alpha - r_1^{-2})^{1/2}(2\alpha - r^{-2})^{1/2}}{2\alpha - r_1^{-1}r^{-1}}\right) - \frac{4}{\mu}r_2^{-1}(2\alpha - r_2^{-2})^{1/2}\left(\tanh^{-1}\frac{(2\alpha - r_2^{-2})^{1/2}(2\alpha - r_a^{-2})^{1/2}}{2\alpha - r_2^{-1}r_a^{-1}} - \tanh^{-1}\frac{(2\alpha - r_2^{-2})^{1/2}(2\alpha - r^{-2})^{1/2}}{2\alpha - r_2^{-1}r^{-1}}\right) \tag{A1}$$

The corresponding shock asymmetry is reduced to

$$Q_s = r_1 r_2^{-1}\left\{[(2\alpha - r_1^{-2})^{1/2} - (2\alpha - r_a^{-2})^{1/2}] + r_2^{-1}[\tan^{-1}(2\alpha r_a^2 - 1)^{-1/2} - \tan^{-1}(2\alpha r_1^2 - 1)^{-1/2}] + (2\alpha - r_2^{-2})^{1/2}\left[\tanh^{-1}\frac{(2\alpha - r_2^{-2})^{1/2}(2\alpha - r_a^{-2})^{1/2}}{2\alpha - r_2^{-1}r_a^{-1}} - \tanh^{-1}\frac{(2\alpha - r_2^{-2})^{1/2}(2\alpha - r_1^{-2})^{1/2}}{2\alpha - r_2^{-1}r_1^{-1}}\right]\right\} \cdot \left\{[(2\alpha - r_2^{-2})^{1/2} - (2\alpha - r_a^{-2})^{1/2}] + r_1^{-1}[\tan^{-1}(2\alpha r_a^2 - 1)^{-1/2} - \tan^{-1}(2\alpha r_2^2 - 1)^{-1/2}] + (2\alpha - r_1^{-2})^{1/2}\left[\tanh^{-1}\frac{(2\alpha - r_1^{-2})^{1/2}(2\alpha - r_a^{-2})^{1/2}}{2\alpha - r_1^{-1}r_a^{-1}} - \tanh^{-1}\frac{(2\alpha - r_1^{-2})^{1/2}(2\alpha - r_2^{-2})^{1/2}}{2\alpha - r_1^{-1}r_2^{-1}}\right]\right\}^{-1} \tag{A2}$$

In this process, the following integral formula has been used:

$$\int\left(\int \frac{v(2\alpha - v^2)^{1/2}}{(v - v_1)(v - v_2)}\,\mathrm{d}v\right)\mathrm{d}r = (2\alpha r^2 - 1)^{1/2} + (1 - (r_1^{-1} + r_2^{-1})r)\tan^{-1}(2\alpha r^2 - 1)^{-1/2} - \frac{r_1^{-1}(2\alpha - r_1^{-2})^{1/2}}{r_1^{-1} - r_2^{-1}}(r - r_1)\tanh^{-1}\frac{(2\alpha - r_1^{-2})^{1/2}(2\alpha r^2 - 1)^{1/2}}{2\alpha r - r_1^{-1}} + \frac{r_2^{-1}(2\alpha - r_2^{-2})^{1/2}}{r_1^{-1} - r_2^{-1}}(r - r_2)\tanh^{-1}\frac{(2\alpha - r_2^{-2})^{1/2}(2\alpha r^2 - 1)^{1/2}}{2\alpha r - r_2^{-1}}$$

Note that the inverse function of the hyperbolic tangent can be expressed in terms of the logarithmic function

$$\tanh^{-1} t = \frac{1}{2}\ln\frac{1 + t}{1 - t}$$

The shock asymmetry has the following asymptotics:

$$Q_{s_{M\to 1}} = 1,\quad Q_{s_{M\to\infty}} = \frac{1}{8}\frac{-8\sqrt{21} + 10(\tan^{-1}(2/\sqrt{21}) - \pi/2) + 10\sqrt{15}\tanh^{-1}\sqrt{35}/6}{5\sqrt{15} - 4\sqrt{21} + 20(\tan^{-1}(2/\sqrt{21}) - \tan^{-1}(1/\sqrt{15}))} \doteq 1.416$$

The shock distance has the following asymptotics:

$$\Delta_{M\to 1} = \frac{4}{5}\sqrt{\frac{10}{\pi}} \doteq 1.427, \qquad \Delta_{M\to\infty} \to \infty$$

A2 Constant Transport Coefficient Case

For completeness, the analytical solution to the constant case ($s = 0$) is also presented. By recognizing the following integral formula,

$$\int \frac{v}{(v - v_1)(v - v_2)}\,\mathrm{d}v = \frac{1}{v_1 - v_2}(v_1 \ln(v_1 - v) - v_2 \ln(v - v_2))$$

the density solution $r(x)$ can be derived:

$$3\theta_1 M\sqrt{\frac{\gamma\pi}{2}}x = \frac{4}{\mu}\ln\frac{[(r_1^{-1} - r^{-1})/(r_1^{-1} - r_a^{-1})]^{1/r_1}}{[(r^{-1} - r_2^{-1})/(r_a^{-1} - r_2^{-1})]^{1/r_2}} \tag{A3}$$

The corresponding shock asymmetry reduces to

$$Q_s = \frac{\ln[(r_a^{-1} - r_2^{-1})/(r_1^{-1} - r_2^{-1})]^{1/r_2}}{\ln[(r_1^{-1} - r_a^{-1})/(r_1^{-1} - r_2^{-1})]^{1/r_1}} \tag{A4}$$

In this process, the following integral formula has been used:

$$\int\left(\int \frac{v}{(v - v_1)(v - v_2)}\,\mathrm{d}v\right)\mathrm{d}r = \frac{1}{r_1^{-1} - r_2^{-1}}(r_1^{-1}r - 1)\ln(r_1^{-1} - r^{-1}) - \frac{1}{r_1^{-1} - r_2^{-1}}(r_2^{-1}r - 1)\ln(r^{-1} - r_2^{-1})$$

In addition, the shock asymmetry has the following asymptotics:

$$Q_{s_{M\to 1}} = 1, \qquad Q_{s_{M\to\infty}} = \frac{\ln 5^{1/4}}{\ln(5/4)} \doteq 1.803$$

The shock distance has the following asymptotics:

$$\Delta_{M\to 1} = \frac{32}{75}\sqrt{\frac{30}{\pi}} \doteq 1.319, \qquad \Delta_{M\to\infty} \to \infty$$

Acknowledgments

This work was supported by the National Research Foundation of Korea funded by the Ministry of Education, Science and Technology (Basic Science Research Program NRF 2012-R1A2A2A02-046270 and Priority Research Centers Program NRF 2012-048078), South Korea.

References

[1] Becker, R., "Stosswelle und Detonation," *Zeitschrift für Physik*, Vol. 8, No. 1, 1922, pp. 321–362.

[2] Taylor, G. I., and Maccoll, J. W., "Mechanics of Compressible Fluids," *Aerodynamics Theory*, Durand, W. F. (ed.), Vol. 3, Springer, Berlin, 1934.

[3] Morduchow, M., and Libby, P. A., "On a Complete Solution of the One-Dimensional Flow Equations of a Viscous, Heat-Conducting, Compressible Gas," *Journal of the Aeronautical Sciences*, Vol. 16, No. 11, 1949, pp. 674–684, 704.

[4] Mott-Smith, H. M., "Solution of the Boltzmann Equation of a Shock Wave," *Physical Review*, Vol. 82, No. 6, 1951, pp. 885–892. doi:10.1103/PhysRev.82.885

[5] Grad, H., "Profile of a Steady Plane Shock Wave," *Communication on Pure and Applied Mathematics*, Vol. 5, No. 3, 1952, pp. 257–300. doi:10.1002/cpa.3160050304

[6] Al-Ghoul, M., and Eu, B. C., "Generalized Hydrodynamics and Shock Waves," *Physical Review E*, Vol. 56, No. 3, 1997, pp. 2981–2992. doi:10.1103/PhysRevE.56.2981

[7] Myong, R. S., "Thermodynamically Consistent Hydrodynamic Computational Models for High-Knudsen-Number Gas Flows," *Physics of Fluids*, Vol. 11, No. 9, 1999, pp. 2788–2802.

[8] Josyula, E., Vedula, P., and Bailey, W. F., "Kinetic Solution of Shock Structure in a Non-Reactive Gas Mixture," AIAA Paper 2010-817, 2010.

[9] Liepmann, H. W., and Roshko, A., *Elements of Gasdynamics*, Wiley, New York, 1957.

[10] Vincenti, W. G., and Kruger, C. H., *Introduction to Physical Gas Dynamics*, Wiley, New York, 1967.

[11] Gombosi, T. I., *Gaskinetic Theory*, Cambridge Univ. Press, New York, 1994.

[12] Gilbarg, D., and Paolucci, D., "Structure of Shock Waves in the Continuum Theory of Fluids," *Journal of Rational Mechanics and Analysis*, Vol. 2, No. 4, 1953, pp. 617–642. doi:10.1512/iumj.1953.2.52031

[13] Schmidt, B., "Electron Beam Density Measurements in Shock Waves in Argon," *Journal of Fluid Mechanics*, Vol. 39, No. 2, 1969, pp. 361–366. doi:10.1017/S0022112069002229

[14] Alsmeyer, H., "Density Profiles in Argon and Nitrogen Shock Waves Measured by the Absorption of an Electron Beam," *Journal of Fluid Mechanics*, Vol. 74, No. 3, 1976, pp. 497–513. doi:10.1017/S0022112076001912

[15] Boyd, I. D., "Analysis of Rotational Non-Equilibrium in Standing Shock Waves of Nitrogen," *AIAA Journal*, Vol. 28, No. 11, 1990, pp. 1997–1999. doi:10.2514/3.10511

[16] Zhong, X., MacCormack, R. W., and Chapman, D. R., "Stabilization of the Burnett Equations and Applications to Hypersonic Flows," *AIAA Journal*, Vol. 31, No. 6, 1993, pp. 1036–1043. doi:10.2514/3.11726

[17] Woo, M., and Greber, I., "Molecular Dynamics Simulation of Piston-Driven Shock Wave in Hard Sphere Gas," *AIAA Journal*, Vol. 37, No. 2, 1999, pp. 215–221. doi:10.2514/2.692

[18] Xu, K., "Gas-Kinetic BGK Scheme for the Navier–Stokes Equations and Its Connection with Artificial Dissipation and Godunov Method," *Journal of Computational Physics*, Vol. 171, No. 1, 2001, pp. 289–335. doi:10.1006/jcph.2001.6790

[19] Myong, R. S., "Computational Method for Eu's Generalized Hydrodynamic Equations of Rarefied and Microscale Gasdynamics," *Journal of Computational Physics*, Vol. 168, 2001, pp. 47–72. doi:10.1006/jcph.2000.6678

[20] Myong, R. S., "Generalized Hydrodynamic Computational Model for Rarefied and Microscale Diatomic Gas Flows," *Journal of Computational Physics*, Vol. 195, No. 2, 2004, pp. 655–676. doi:10.1016/j.jcp.2003.10.015

[21] Cai, C., Liu, D. D., and Xu, K., "One-Dimensional Multiple-Temperature Gas-Kinetic Bhatnagar Gross Krook Scheme for Shock Wave Computation," *AIAA Journal*, Vol. 46, No. 5, 2008, pp. 1054–1062. doi:10.2514/1.27432

[22] Iannelli, J., "Implicit Galerkin Finite Element Runge–Kutta Algorithm for Shock Structure Investigations," *Journal of Computational Physics*, Vol. 230, No. 1, 2011, pp. 260–286. doi:10.1016/j.jcp.2010.09.025

[23] Roy, C. J., McWherter-Payne, M. A., and Oberkampf, W. L., "Verification and Validation for Laminar Hypersonic Flowfields, Part 1: Verification," *AIAA Journal*, Vol. 41, No. 10, 2003, pp. 1934–1943. doi:10.2514/2.1909

[24] Fogiel, M., *Handbook of Mathematical, Scientific, and Engineering: Formulas, Tables, Functions, Graphs, Transforms*, Research and Education Assoc., NJ, 1997.

X. Zhong
Associate Editor